JOURNAL OF ENERGY SYSTEMS

2023, 7(4)

2602-2052 DOI: 10.30521/jes.1097439 Research Article

# Numerical study on ground-air heat exchanger performance in a hot climate under different inlet air temperatures

Ali Naser Hussien *

University of Technology, Biomedical Engineering Department, Baghdad, IRAQ, ali.n.hussien@uotechnology.edu.iq

Submitted: 04.04.2023
Accepted: 15.08.2023
Published: 31.12.2023

* Corresponding Author

**Abstract:** The present study includes a numerical assessment of air-cooling by EAHE (i.e., Earth to Air Heat Exchanger) on hot days in Baghdad city. EAHE consists of pipes buried in a certain depth in the soil, where the temperature is moderate throughout the year. The effect of different input air temperatures at day and night on the EAHE performance has been studied, taking into account the change in soil temperature due to continuous passing of hot air causing an increase in soil temperature and lowers its cooling capacity. In Baghdad (i.e. capital of Iraq), the hot days are extended from mid-April to mid-October. During these months, the weather is characterized by the high solar intensity at day with a daily range exceeding 15 °C. Ambient air temperature varies greatly through spring, summer, and autumn. The various ambient temperatures recorded and documented for Baghdad are used as the inlet temperatures of EAHE in the present study. Besides, the pressure drops and power losses through pipes have been studied, too. The simulated results indicates that the use of EAHE gives the accepted outlet temperature for space cooling (about 26 ℃) on hot days of spring and autumn. In addition, the decrease of ambient temperature less than soil temperature at night leads to lessening the heat storage in soil.

***Keywords:*** *EAHE design, Geothermal cooling, Passive cooling in Baghdad city, Renewable energy*

Cite this paper as: Hussein, A.N., Numerical study on ground-air heat exchanger performance in a hot climate under different inlet air temperatures. *Journal of Energy Systems 2023; 7*(4): 315-326, DOI: 10.30521/jes.1097439



| | **Nomenclature** | | | Greek symbols | |
|---|---|---|---|---|---|
| $A$ | Area | $Pr$ | Prandtl number | $\alpha$ | Thermal diffusivity |
| $As$ | Ambient variation amplitude | $Q$ | Heat energy | $\rho$ | Density |
| $c$ | Specific heat capacity | $R$ | Thermal resistance | $\mu$ | Dynamic viscosity |
| $d$ | Diameter | $Re$ | Reynolds number | Subscript | |
| $h$ | Convective heat transfer coefficient | $r$ | Radius | $r$ | Radial direction |
| $i, j$ | Control units in axial and axial direction | $T$ | Temperature | $s$ | Soil |
| $k$ | Thermal conductivity | $t$ | Time | $x$ | Axial direction |
| $\dot{m}$ | Mass flowrate | $v$ | Velocity | Abbreviation | |
| $Nu$ | Nusselt number | $x$ | Axial distance | CFD | Computational fluid dynamics |
| $p$ | Pipe perimeter | $z$ | Underground depth | EAHE | Earth to air heat exchanger |

## 1. INTRODUCTION

Earth to Air Heat Exchanger (EAHE) is one of the geothermal energy applications that is considered a renewable clean energy resource. It is a very simple way for space heating or cooling, since it needs only an airflow through a buried underground pipe, where the earth works as a large heat source on cold days and large heat sink on hot days. Many works studied the influence of the design parameters on EAHE performance. For instance, Gooroochurn et al., [1] was achieved a drop in air temperature by 5 ℃ and 8 ℃ when the air velocity was 2.3 m/s and 4 m/s respectively. Promised results was obtained about the air temperature difference through the EAHE as reported by Lattieff [2]. Sehli et al., [3] proposed a steady one-dimensional numerical model for the cooling performance of EAHE, at various depths. They explored the Reynolds number, and length to diameter ratio effects on the EAHE performance. Their results indicated that, as the depth and length to diameter ratio increase, the air-temperature drop increases, and increasing the Reynolds number decreases the air-temperature drop. In addition, they stated that the use of EAHE alone is insufficient for the thermal comfort in south Algeria without combining it with other type of air-conditioning ways. Mihalakakou et al., [4,5] studied the influence of EAHE pipe diameter on the air-temperature drop and found that, as the pipe diameter was increased, the air-temperature drop and the heat transfer coefficient of convection were decreased. Ahmed et al., [6] examined the effects of length, depth, pipe diameter, pipe material, and airflow velocity on the EAHE performance. They found that the pipe length had a major effect compared with the other parameters. On the other hand, other papers concerned with a so-called soil saturation analysis. They reported one of the drawbacks of the heat stored in the ground in summer/heat absorbed from the ground in winter due to continuous flow of ambient air through a buried pipe. In general, this effect decreases the earth-air temperature difference (i.e., decreases the soil temperature near the pipe wall from the air temperature), and then decreases the benefit of EAHE usage. This drawback mainly depends on the rate of heat exchanged. In a different work, Rouag, et al., [7] studied the deterioration of the EAHE due to the continuous operation and soil thermal saturation by using the method of Bessel function, and testing the operation at an outdoor air temperature of 57 $^{o}$C. They concluded that the soil radius or the heated soil thickness around the EAHE pipe after 6 hours of operation was able to exceed 0.55 m. These results were validated experimentally by Mehdid et. al., [8] with an estimation of the air temperature inside the EAHE pipe. The results indicated a good agreement between the two studies. The transient analytical model of EAHE proposed by Krarti and Kreider [9] indicated that a few days were required to obtain a periodic steady-state operation of EAHE system. Paepe and Janssens [10] introduced a 1D model to analyze the design parameter and their effects on heat transfer and hydraulic performance of EAHE. Hollmuller [11] developed a complete solution that included a heat diffusion through a cylindrical shape of the soil-air heat exchanger, the study assumed constant harmonic temperature at the input. In a simple accurate heat exchanging approach to compute the underground temperature at various depths proposed by Badescu [12], the limit of cooling and heating of a system was estimated by using the actual climatic conditions. In Ref. [13], the authors conducted numerical analysis and experimental validation of an EAHE, which was used to decrease the space energy consumption for heating and cooling demands of buildings by using the ground energy storage. They solved the heat balance equation with turbulent flow numerically by a commercial CFD tool (FLUENT), which contained a Reynolds stress model as a turbulence model. The maximum difference between numerical and experimental validation results did not exceed 15%.

A review paper of Bhutta et al., [14] concerned the important roles of CFD applications in EAHE performance analysis and determining their thermal behavior. Wu et al., [15] used a transient implicit model dependent on a CFD study with a numerical approach of heat transfer to estimate the performance and cooling capacity of the EAHE system. The experimental results gave about 74.6 kWh of cooling capacity per day.

Misra et al., [16] studied experimentally and numerically various parameters affecting the EAHE performance such as the thermal conductivity of the soil, airflow velocity, continuous work durations, and pipe diameter by using a CFD software. Their study presented the significant effects of the transient conditions on the EAHE operation. In Ref. [17], the experimental explorations clarified that the maximum deterioration in the thermal performance in terms of temperature drop obtained during continuous operation of 24 hours in a work on the thermal saturation and recovery of soil around the EAHEs pipes. Laknizi et al., [18] conducted an EAHE model for a poultry house heating and cooling. The model explored the effects of air velocity, tube diameter, and physical properties on the temperature drop. The results indicated that a higher efficiency with a good coefficient of performance could be obtained at an air velocity 2 m/s in a pipe with 100 mm diameter and 30 m length. Verma et al., [19] introduced a useful detailed review with many studies took care of different effects and parameters related to EAHE performance, and advised to couple the EAHE system with other wind turbine or solar baskets, etc., to optimize the performance.

In the present work, a 2D unsteady heat transfer model will be applied on the control volume of EAHE and mathematically solved. The effects of various inlet air temperatures on the output temperature and on the soil thermal saturation will be calculated for Baghdad city. Besides, the effect of different design parameters, (length, diameter, air flowrate) on the output temperature will be tested. The long summer in Baghdad can be divided into three periods; moderate-hot period, hot period, and very hot (harsh) period. The average maximum ambient temperatures at day, minimum ambient temperatures at night, and the extreme maximum temperature recorded for the last years in Baghdad [20] are indicated in Table 1.

*Table 1. Monthly average temperatures in Baghdad in last five years (℃) [20].*

| Moderate-hot period | | | Hot period | | | Very hot period | | |
|---|---|---|---|---|---|---|---|---|
| 15 Apr.-15 May-21 Sep.-15 Oct. | | | 16 May- 10 Jun.-1-20 Sep. | | | 11 Jun.- 31 Aug. | | |
| $T_{min}$ | $T_{max}$ | $T_{max/}$ Extr. | $T_{min}$ | $T_{max}$ | $T_{max/}$ Extr. | $T_{min}$ | $T_{max}$ | $T_{max/}$ Extr. |
| 17 | 36 | 40 | 23 | 41 | 44 | 28 | 47 | 52 |

The lack of required data about this type of renewable energy deprives many buildings in Iraq of using it and led to using of traditional devices such as the compression cycle devices in air-conditioning, which forms a high load on electricity supply networks. The present study indicates the extent and how to benefit from the EAHE in Baghdad along the hot days, taking into account, a number of overlapping influences, such as the inlet air temperatures that change during the hours of a day and during the hot season, in addition to the amount of air and the dimensions of the EAHE. The objectives of the present study can be summarized by:

Filling the lack of data on the possibility of using EAHE in air cooling in Baghdad and studying the effects of diameter, air mass flowrate, and pipe length on the outlet temperature, pressure drop and power losses due to friction in EAHE.

Calculation of the EAHE outlet temperatures for the various inlet temperatures at the selected days along the hot months, in Baghdad and determine the most appropriate days for using the EAHE.

Study the effects of high inlet air-temperatures recorded in summer and the low inlet air temperatures recorded at night of spring and autumn on the soil thermal saturation and on the cooling capacity of EAHE.

## 2. EAHE CALCULATIONS

The ground undisturbed temperature that is a function of year day and the depth from the surface can be calculated as from Ref. [21] as,

$$T_{z,t} = T_m - A_s exp\left[-z\left(\frac{\pi}{365\alpha_s}\right)^{(0.5)}\right] cos\left\{\frac{2\pi}{365}\left[t - t_o - \frac{z}{2}\left(\frac{365}{\pi\alpha_s}\right)^{(0.5)}\right]\right\}. \quad (1)$$

Here, $T_{z,t}$ is the temperature of the soil at time $t$ (sec) and the depth $z$ (m). $T_m$ is the average of ambient temperature through the year (24 °C) according to Ref. [2], $A_s$ is the ambient variation amplitude (°C), $\alpha_s$ is the thermal diffusivity of the soil ($m^2/s$; $m^2/day$), $t$ is the time beginning from January 1 (day), and $t_o$ is the time constant ground surface.

As the air passes through the EAHE pipes, the heat exchanges continuously between the air and the soil, the temperature of soil near the pipe wall becomes higher than that calculated by Eq. 1 and called disturbed temperatures. Therefore, the unsteady state model is required to analyze the soil temperature variation by heat balance method; the computing domain of soil around the pipe can be divided into a number of control units of a torus shape as shown in Fig. 1. The adjacent control units are connected to each other. The following assumptions are required to build the mathematical model of temperature variation Niu et al., [17]:

*1) The undisturbed temperature is the initial temperature of ground soil and air.*
*2) Incompressible and turbulent airflow inside EAHE pipe.*
*3) The air and soil thermal properties are constant.*
*4) The pipe thickness is so small and its thermal resistance is ignored.*
*5) Ignoring the depth effects on soil disturbed temperature around the pipe.*
*6) Symmetrical heat transfer in circumferential direction.*

To express the heat transfer between air and soil in EAHE, a 2D transient heat conduction equation in cylindrical coordinates (where the axial direction is $x$ and the radial one is $r$) as:

$$\frac{\rho c_s}{k_s}\left(\frac{\partial T}{\partial t}\right) = \frac{\partial^2 T}{\partial x^2} + \frac{\partial}{r\partial r}\left(r\frac{\partial T}{\partial r}\right) \quad (2)$$

where ρ, $c_s$, and $k_s$ represent the soil density, specific heat capacity, and thermal conductivity respectively. By dividing the disturbed region around the pipe into $M$ division elements of length $\Delta x$ in $x$-direction, and $N$ division elements of length $\Delta r$ in $r$-direction. The disturbed temperature as a function of $x$, $r$ and time $t$ is $T(x, r, t)$, and the boundary and initial conditions corresponding to Eq. 2 become:

$$T(0, r, t) = T(M, r, t) = T_{undisturbed}, T(x, 0, t) = T_{air}, T(x, N, t) = T_{undisturbed}, T(x, r, 0) = T_{undisturbed} \quad (3)$$

Assume each torus shape division of disturbed region has a control unit ($i$, $j$) and the adjacent divisions in $x$ direction have control units ($i$-1, $j$) and ($i$+1, $j$), whereas the adjacent divisions in $r$ direction have control units ($i$, $j$-1) and ($i$, $j$+1) (see Fig. 1). Denoting the mid-point temperature of this control unit at time $t$ as $T_{i,j}^t$, also their thermal resistances in the x-direction $R_{i,j}^x$ and in $r$ direction $R_{i,j}^r$ can be calculated as in Ref. [22]:

$$R_{i,j}^x = \frac{\Delta x}{\pi k(r_j^2 - r_{j-1}^2)} \quad (4)$$

$$R_{i,j}^r = \frac{\ln\left(\frac{r_j}{r_{j-1}}\right)}{2\pi k\Delta x} \quad (5)$$

$C_{i,j}$ is the heat capacity of the soil unit ($i$, $j$), can be calculated as Athienitis and Santamouris [23]:

$$C_{i,j} = \pi\,\Delta x\left[(r_j)^2 - (r_{j-1})^2\right]\rho\, c_s \quad (6)$$

Therefore, Eq. 2 can be discretized by finite difference method with combination of the thermal resistances and soil heat capacity mentioned above. The differenced form of Eq. 2 to calculate the instantaneous temperature of the control unit ($i$, $j$) can be written as in Ref. [17]:

$$T_{i,j}^{t+1} = \frac{\Delta t}{C_{i,j}}\left(\frac{T_{i+1,j}^{t} - T_{i,j}^{t}}{(R_{i+1,j}^{x} + R_{i,j}^{x})/2} + \frac{T_{i-1,j}^{t} - T_{i,j}^{t}}{(R_{i-1,j}^{x} + R_{i,j}^{x})/2} + \frac{T_{i,j+1}^{t} - T_{i,j}^{t}}{(R_{i,j+1}^{r} + R_{i,j}^{r})/2} + \frac{T_{i,j-1}^{t} - T_{i,j}^{t}}{(R_{i,j-1}^{r} + R_{i,j}^{r})/2}\right) + T_{i,j}^{t} \quad (7)$$

Besides, the differenced form of Eq. 2 for the boundary units can be written as follows when $i$=1:

$$T_{i,j}^{t+1} = \frac{\Delta t}{C_{i,j}}\left(\frac{T_{i+1,j}^{t} - T_{i,j}^{t}}{(R_{i+1,j}^{x} + R_{i,j}^{x})/2} + \frac{T_{undis} - T_{i,j}^{t}}{R_{i,j}^{x}} + \frac{T_{i,j+1}^{t} - T_{i,j}^{t}}{(R_{i,j+1}^{r} + R_{i,j}^{r})/2} + \frac{T_{i,j-1}^{t} - T_{i,j}^{t}}{(R_{i,j-1}^{r} + R_{i,j}^{r})/2}\right) + T_{i,j}^{t} \quad (8)$$

when $i$ =M

$$T_{i,j}^{t+1} = \frac{\Delta t}{C_{i,j}}\left(\frac{T_{undis} - T_{i,j}^{t}}{R_{i,j}^{x}} + \frac{T_{i-1,j}^{t} - T_{i,j}^{t}}{(R_{i-1,j}^{x} + R_{i,j}^{x})/2} + \frac{T_{i,j+1}^{t} - T_{i,j}^{t}}{(R_{i,j+1}^{r} + R_{i,j}^{r})/2} + \frac{T_{i,j-1}^{t} - T_{i,j}^{t}}{(R_{i,j-1}^{r} + R_{i,j}^{r})/2}\right) + T_{i,j}^{t} \quad (9)$$

when $j$ = 1

$$T_{i,j}^{t+1} = \frac{\Delta t}{C_{i,j}}\left(\frac{T_{i+1,j}^{t} - T_{i,j}^{t}}{(R_{i+1,j}^{x} + R_{i,j}^{x})/2} + \frac{T_{i-1,j}^{t} - T_{i,j}^{t}}{(R_{i-1,j}^{x} + R_{i,j}^{x})/2} + \frac{T_{i,j+1}^{t} - T_{i,j}^{t}}{(R_{i,j+1}^{r} + R_{i,j}^{r})/2} + \frac{T_{air,i}^{t} - T_{i,j}^{t}}{R_{i,j}^{r}}\right) + T_{i,j}^{t} \quad (10)$$

When $j$ = $N$

$$T_{i,j}^{t+1} = \frac{\Delta t}{C_{i,j}}\left(\frac{T_{i+1,j}^{t} - T_{i,j}^{t}}{(R_{i+1,j}^{x} + R_{i,j}^{x})/2} + \frac{T_{i-1,j}^{t} - T_{i,j}^{t}}{(R_{i-1,j}^{x} + R_{i,j}^{x})/2} + \frac{T_{undis} - T_{i,j}^{t}}{R_{i,j}^{r}} + \frac{T_{i,j-1}^{t} - T_{i,j}^{t}}{(R_{i,j-1}^{r} + R_{i,j}^{r})/2}\right) + T_{i,j}^{t} \quad (11)$$

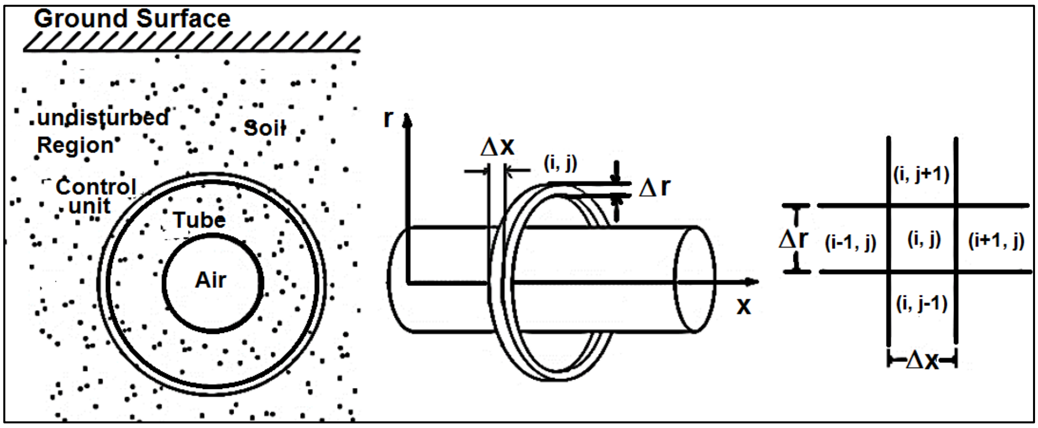

*Figure 1. Governing unit structure of EAHE tube with soil around it in cylindrical coordinates.*

Paepe and Janssens [8] give the heat removed from ambient air through a pipe as:

$$Q_c = \dot{m}\, c_p (T_{in} - T_{out}) \quad (12)$$

where $\dot{m}$ represent the airflow rate (kg/s), $c_p$ is the specific heat capacity of air (J/kg-K), $T_{in}$, and $T_{out}$ are the temperature of the air at the inlet and the outlet of EAHE pipe respectively in (°C).

The above rate of heat transfer is absorbed by the soil around pipe wall and can be calculated by Ref. [8]:

$$Q_c = hA\Delta T_{lm} \quad (13)$$

where $h$ is the coefficient of heat transfer by convection (W/m$^2$-K), A is the surface area of the pipe (m$^2$), and $\Delta T_{lm}$ is the logarithmic mean temperature difference that is given by.

$$\Delta T_{lm} = (T_{in} - T_{out})/ln\left[\frac{(T_{in} - T_{wall})}{(T_{out} - T_{wall})}\right] \quad (14)$$

By eliminating $Q_c$ from Eqs. (12) and (13) and substituting $\Delta T_{lm}$ of Eq. 14 in Eq. 13, the air temperature at the EAHE pipe outlet can be calculated in exponential form as follows:

$$T_{out} = T_{wall} + (T_{in} - T_{wall})exp\,(-hA/\dot{m}\,c_p) \quad (15)$$

In the differentiation with substitute surface area ($A$) by pipe perimeter ($p$) multiplied by the derivative of distance ($x$), we obtain:

$$T_{air}(i+1) = T_{wall}(i) + (T_{air}(i) - T_{wall}(i))exp\,(-hpx/\dot{m}\,c_p) \quad (16)$$

The coefficient of convective heat transfer h can be calculated as follows Holman, [20]:

$$h = Nu\,k_{air}/d \quad (17)$$

where $k_{air}$ is the air thermal conductivity, and $Nu$ is the Nusselt number calculated for cooling operation as in Refs. [24] and [25]:

$$Nu = 0.023\,Re^{0.8}Pr^{0.3} \quad (18)$$

Here $Re$ and $Pr$ are the Reynolds number and Prandtl number, respectively. They are given by,

$$Re = \rho_{air}vd/\mu, Pr = \mu c_p/k_{air} \quad (19)$$

Here $\rho_{air}$, $v$, $d$, and $\mu$ are air density, air velocity, diameter, and is absolute viscosity of air, respectively. The pressure drop through the pipe of EAHE due friction, assuming a smooth inner pipe wall [26]:

$$\Delta p = f\rho_{air}\frac{L}{d}\frac{v^2}{2} \quad (20)$$

where $f$ is the friction factor which is calculated as,

$$f = 64/Re \quad if \quad Re < 2300 \quad (21)$$

and

$$f = (1.82\,log\,Re - 1.64)^{-2} \quad if \quad Re \geq 2300 \quad (22)$$

Most of the airflow types in EAHE are turbulent flow, where $Re$ is very greater than 2300. The power losses through the pipe due the friction can be calculated as,

$$P_f = \Delta p\,\dot{V} \quad (23)$$

## 3. RESULTS AND DISCUSSIONS

In the present study, the EAHE outlet temperature is calculated by using the transient mathematical model indicated above. The Matlab software is used in order to solve the equations. The input data used are the inlet air temperature to EAHE, which are the actual ambient temperatures that hourly recorded in Baghdad for 4 days that selected to represent the 3 weather periods indicated in Table 1. These 4 days are April 25, May 25, July 22, and September 22. These days are assumed to be repeated periodically for several days later. This assumption is essential with the continuous operation of EAHE to find the time required to reach the steady-state outlet air temperature or the soil temperature saturation. The air and soil properties are indicated in Table 2. The initial soil temperatures are calculated from Eq. 1 and shown in Fig. 2. The design parameters chosen for theoretical simulation are the pipe diameter of 10 cm, 20 cm, and 30 cm and for each diameter the air mass flow rates are taken as 0.05 kg/s, 0.1 kg/s, and 0.15 kg/s, and the pipe depth is 3 m.

*Table 2. The thermo-physical properties of air and soil.*

| Material | Density (kg/m$^3$) | Specific heat (J/kg ℃) | Thermal conductivity (W/m ℃) |
|---|---|---|---|
| Air | 1.225 | 1006 | 0.0242 |
| Soil | 2050 | 1840 | 0.52 |

The results of Figs. 3-6 show the ambient temperature, and the EAHE outlet air temperatures after a 50 m length from inlet, and 3 m pipe depth, for the pipe diameters of 10 cm, 20 cm, and 30 cm. Note that the air mass flow-rate for each diameter are 0.05 kg/s, 0.1 kg/s, and 0.15 kg/s with the associated dates. It is clear that the drop in air temperature increases as the diameter decreases, also for the same diameter, as the air mass flow-rate increases, the temperature drop decreases, due to the increase in air velocity, which decreases the time required for heat exchange.

The ambient temperatures of April 25 shown in Fig. 3, are assumed to be repeated for the next days, these temperatures are between 36.3 ℃ and 17.5 ℃, whereas the undisturbed soil temperature is 23.27 ℃. This means that air is heated at night hours when the ambient temperatures are less than the undisturbed soil temperature, and this effect contributes in decreasing the soil heat storage, therefore, the daily increase in the outlet temperature of EAHE due to continuous operation, is very low and it does not exceed the temperature 0.5 ℃.

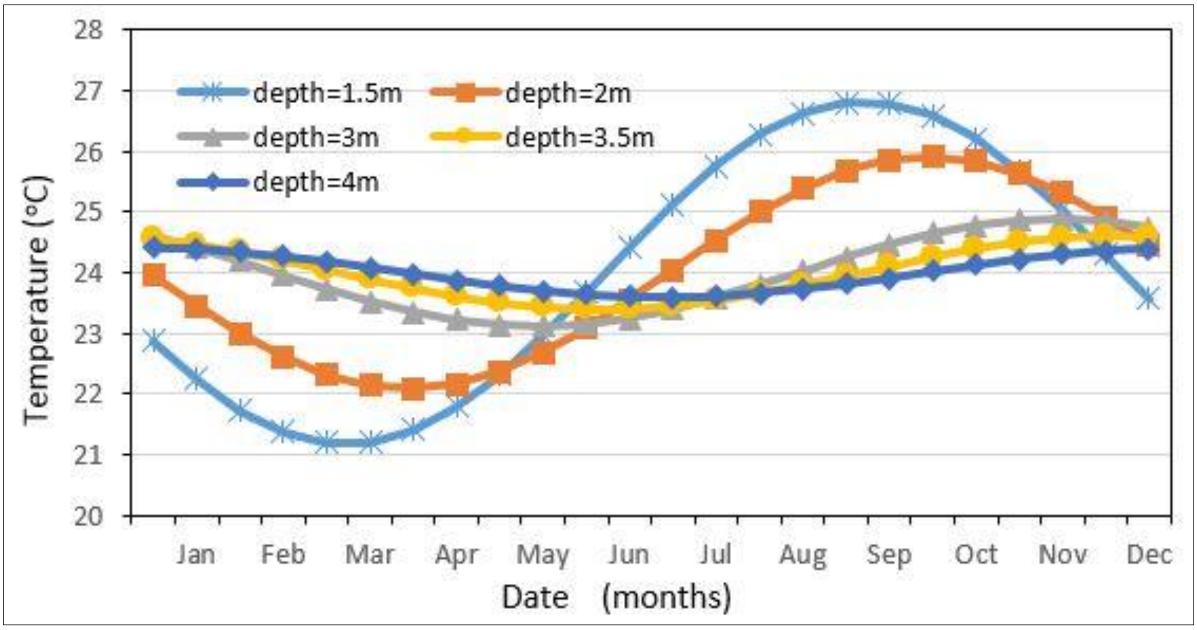


*Figure 2. Monthly variation of the soil temperature at different depth in Baghdad.*

Similar behavior occurred in the last days of September as shown in Fig. 6. The maximum and minimum temperatures in these days are 39.6 and 18.3 ℃, respectively, and the undisturbed soil temperature is 24.5 ℃. The outlet temperatures in Figs. 3 and 6 represent the outlet temperatures of EAHE after 50 m length from inlet for the moderate-hot weather period, the drop in maximum ambient temperature are about 10 ℃, 8 ℃, and 7 ℃ for pipe diameter 10 cm, 20 cm, and 30 cm, respectively. The outlet air temperature from 10 cm pipe dimeter is suitable for cooling demand for all mass flowrate simulated along the day and for the diameter of 20 cm, except some hours at noon, whereas the outlet temperatures exceeded 30 ℃ for more than 7 hours through day time, when the pipe diameter is 30 cm. The ambient temperatures of the hot period represented by the last days of May are between the maximum temperature of 39 ℃ and minimum temperature of 25 ℃ as shown in Fig. 4 with the outlet air temperatures of EAHE. The values of the outlet air temperature of pipe diameter of 10 cm meet the cooling demand of spaces to some extent but for other diameters are not. The increase in outlet temperatures due to continuous operation is attenuated by the moderate ambient temperatures at night.

As an example of a very hot period the ambient temperatures of the last days of July are shown in Fig. 5 with the outlet air temperature of EAHE after 50 m from the inlet, clearly from the figure that the outlet temperatures of all diameters and mass flowrates are unsatisfied the cooling requirement of spaces. On the other hand, the heat storage in the soil is increased continuously with continuous operation of EAHE, therefore the average increase of outlet temperature of the seventh day with respect to the first day is about 3 ℃. This means that the continuous operation of EAHE in very hot period is useless, and may be useful to operate at night only.

The variations of air temperatures along the pipe of EAHE for the 10 cm and 20 cm pipe diameters simulated are shown in Fig. 7, when the inlet temperatures are 32 ℃ at 6 AM and 51 ℃ at 1 PM of July 22, and 17.5°C at 5 AM of April 25. The greater temperature drops are occurred at the beginning of the pipe due to high heat exchange that results from the high temperature difference between the air and the soil and decreases individually with increasing the length in proportion with the temperature difference decreases. In addition, it is clearly that the inlet air of 17.5°C at 5 AM of April 25 is heated because its temperature is lower than the soil temperature. The air temperatures for all inlet conditions and pipe diameters are closed to soil temperature as the length increases.

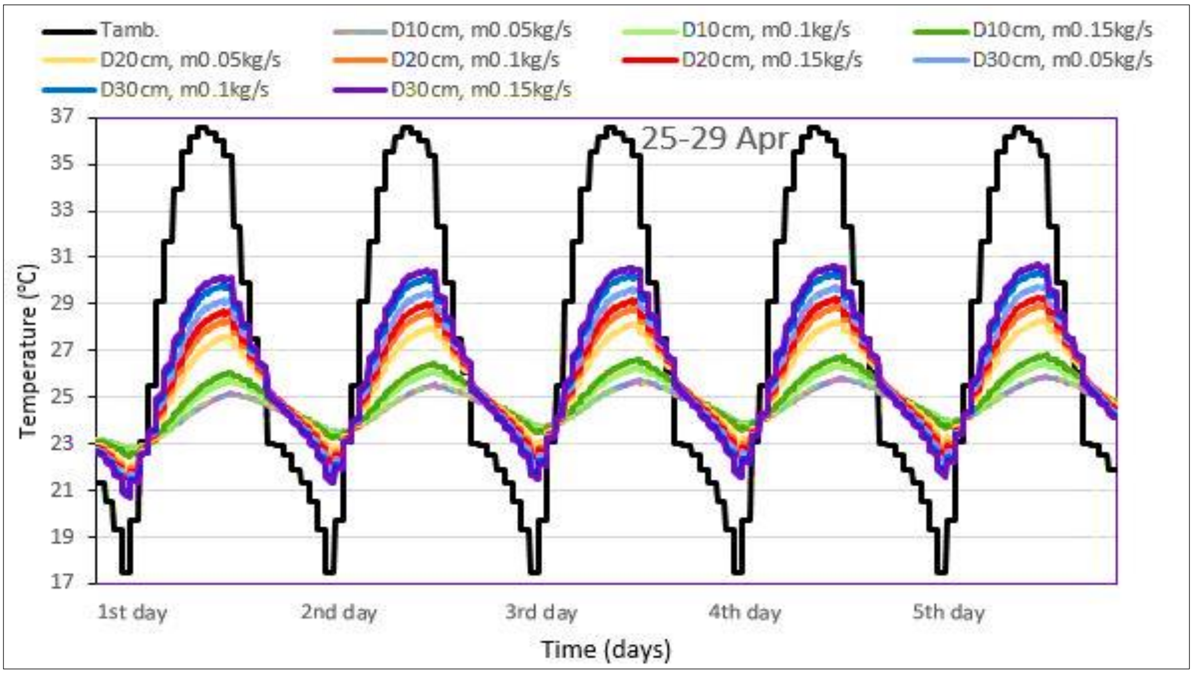


*Figure 3 EAHE outlet temperature variations and ambient temperature from 25 to 29 April for different diameters and air mass flowrates at 3 m pipe depth.*

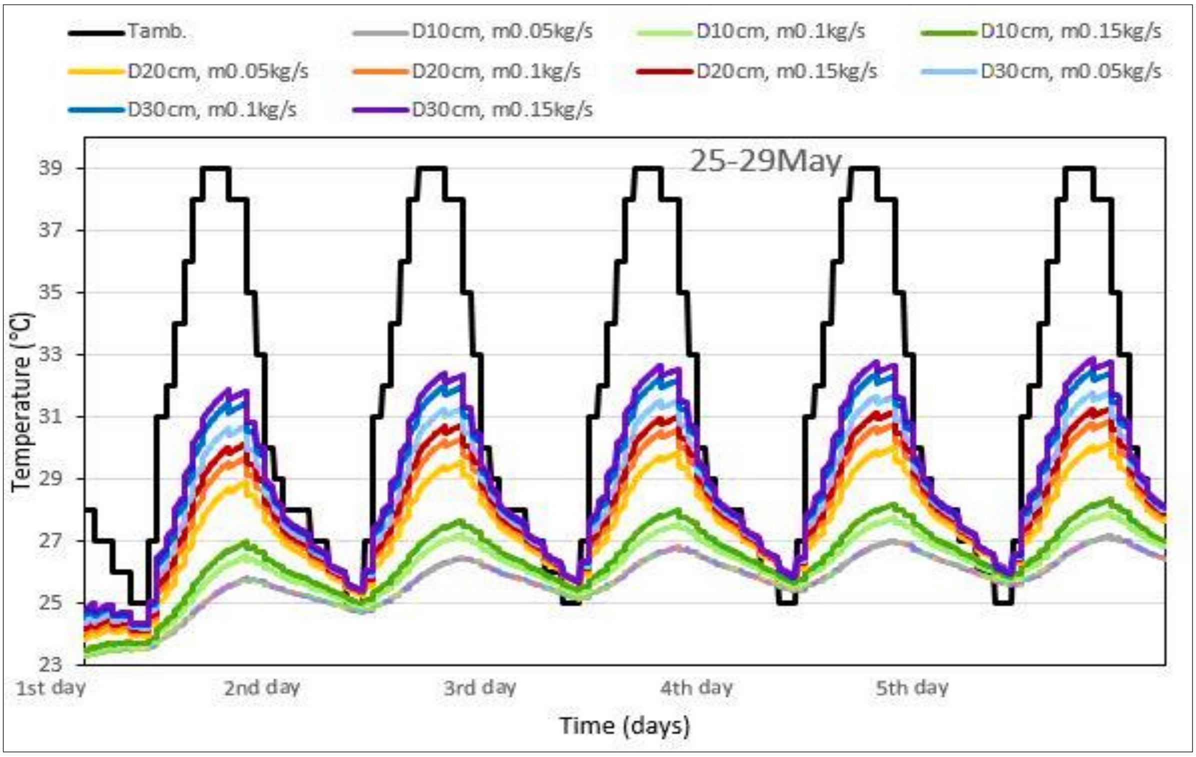


*Figure 4. EAHE outlet temperature variations and ambient temperature from 25 to 29 May for different diameter and air mass flowrates at 3 m pipe depth.*

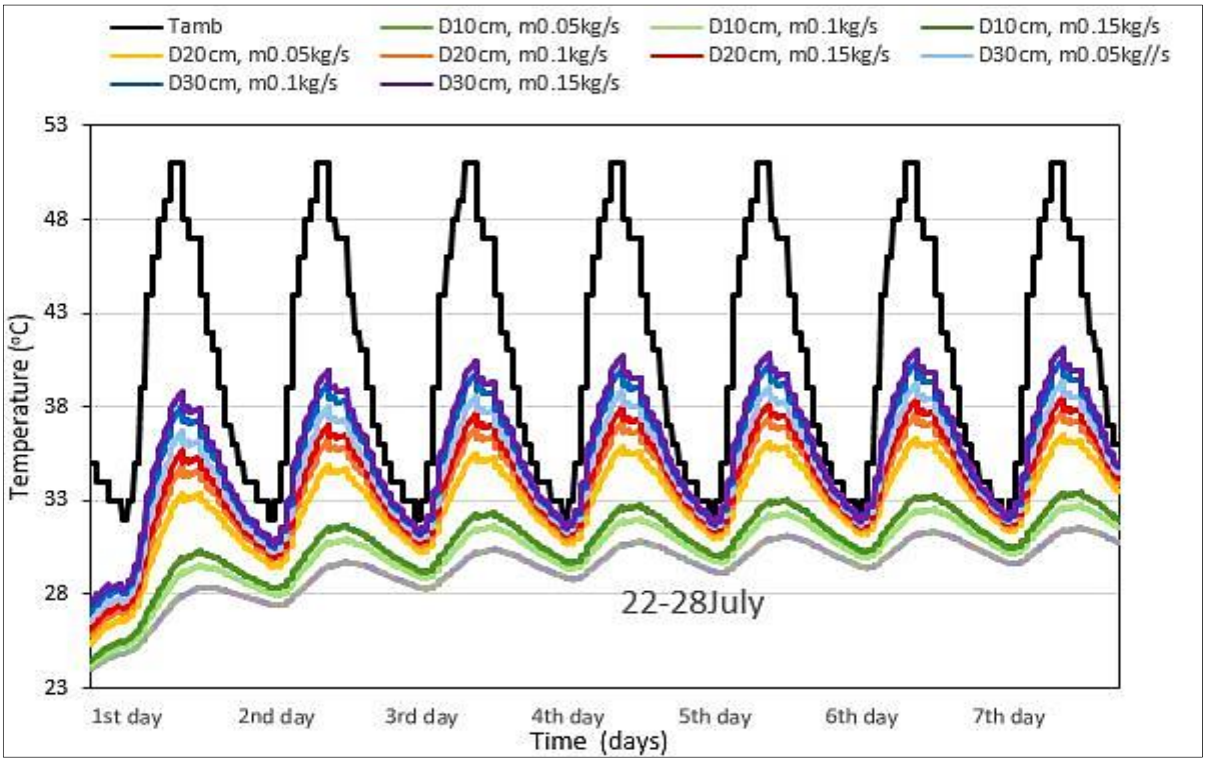


*Figure 5. EAHE outlet temperature variations and ambient temperature from 22 to 28 July for different diameters and air mass flowrates at 3 m pipe depth.*

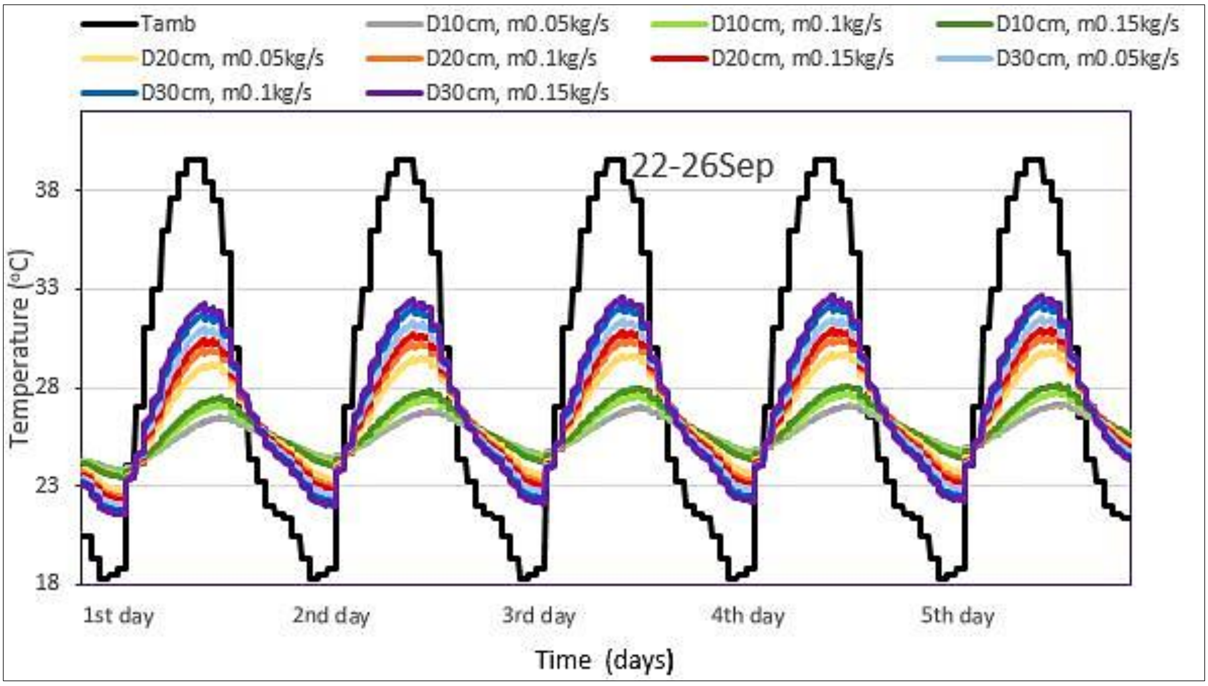


*Figure 6. EAHE outlet temperature variations and ambient temperature from 22 to 26 Sep for different diameters and air mass flowrates at 3 m pipe depth.*

On the other hand, the effect of the increase of pressure drops and power losses with the increase of air flowrate are shown in Figs. 8, and 9 respectively.

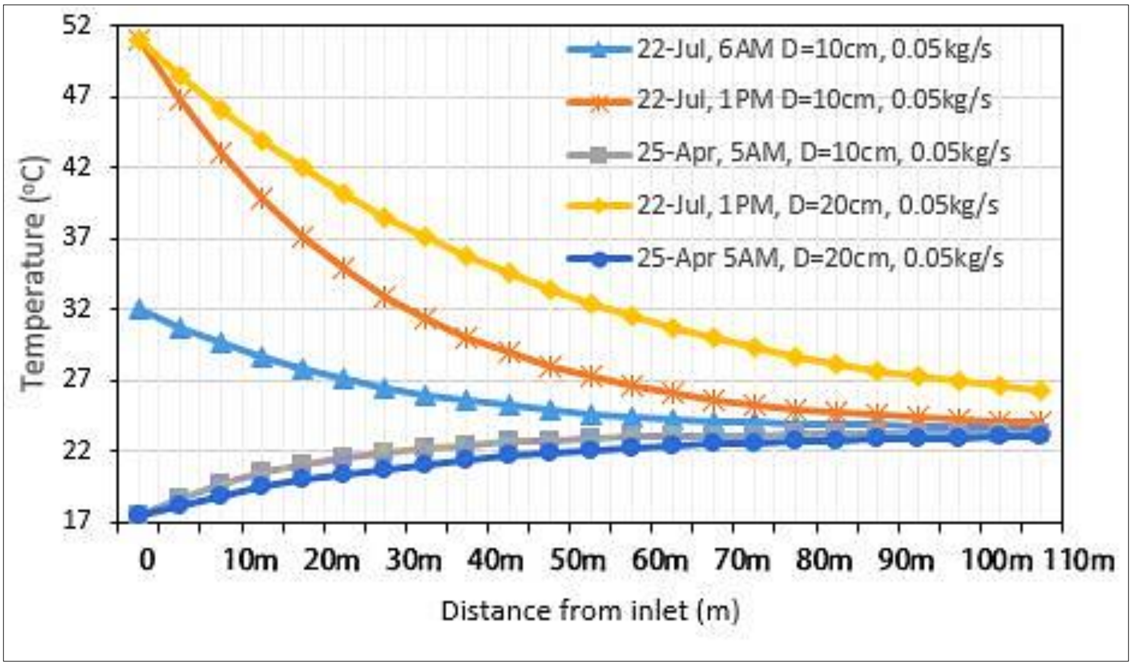


*Figure 7 The variation of air temperature in EAHE along the pipe length at 3m pipe depth*

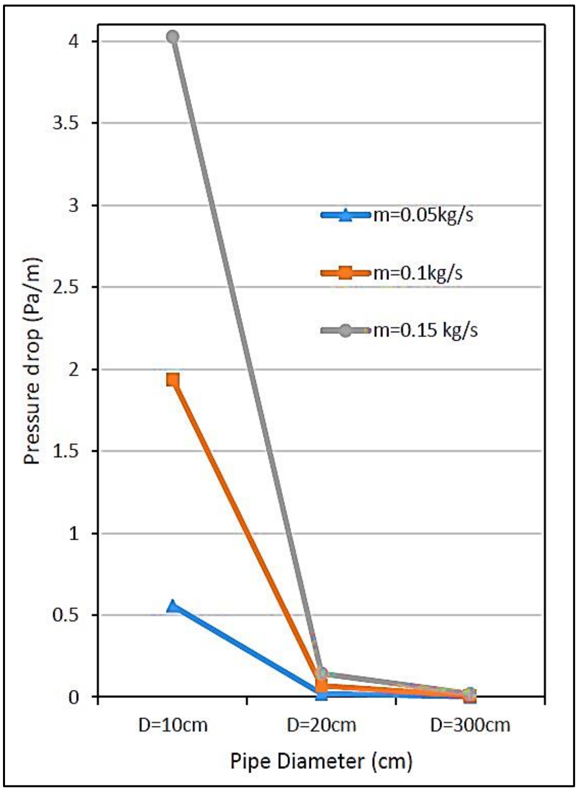


*Figure 8. The pressure drops through EAHE due friction.*

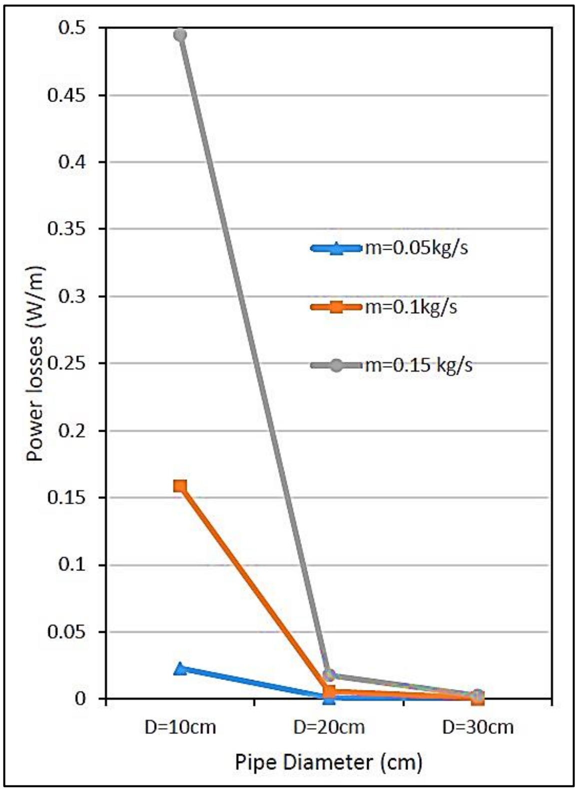


*Figure 9. The air power losses through EAHE due friction.*

## 4. CONCLUSION

The conclusions of the present study can be concentrated about two main points: The first is related to the temperature drop in EAHE that increases as the pipe diameter decreases. In addition, for the same diameter, the mass flow-rate decreases when the temperature drop increases, too. The maximum air temperature drop occurred at the beginning of EAHE and the air temperature is closed to soil temperature as the pipe length increases. A horizontal pipe of EAHE of 50 m length after an inlet at 3 m depth gives a useful outlet temperature in a moderate-hot period between April 15 to May 15 and between September 21 to October 15, even with the continuous operation when using a pipe diameter less than 20 cm, and with the mass flow rate less than 0.15 kg/s. In addition, in a hot period between May 16 and June 10 and from the $1^{st}$ to $20^{th}$ of September, when the pipe diameter is less than 10 cm and mass flowrate less than 0.15 kg/s. The outlet temperature at these conditions is less than 28 ℃ and may be used for cooling demand as a clean and energy saving-method. In a very hot period from June 11 to August 31, the temperature drop through EAHE after 50 m from inlet may exceed 20 ℃ according to pipe diameter and mass flow rate, but the outlet temperature remains higher than the space-cooling requirement. The second point is treated with the continuous operation or continuous passing of hot air through the EAHE that increases the outlet temperature of EAHE due to heat storage in soil and the increase in soil temperature near the pipe wall, especially, in a very hot period when the input ambient temperature is high. The large temperature difference between day and night attenuates the soil heat storage, especially, when the input ambient temperature is less than soil temperature, which leads to cooling the soil as it occurs at some night hours of moderate-hot period. The present study can be the beginning and the base for more detailed future works, for instance, studying the intermittent operation of EAHE for recovering the soil cooling capacity during a very hot days and determine the reasonable non-working time of EAHE. Besides, the capability of using the EAHE for heating in winter.

**REFERENCES**


[1] Gooroochurn, M., Mungur, M., Shamachurn H., Surnam, B. Y. R., Mandarkhan, F., & Bhoodoo, D., Investigation of the performance of ground-coupled heat exchanger technology for tempering air. Journal of Energy Systems 2022; 6(2): 309-321, DOI: 10.30521/jes.1058233

[2] Lattieff FA, Atiya MA, Lateef RA, Dulaimi A, Jweeg MJ, Abed AM, Mahdi JM and Talebizadehsardari P (2022), Thermal analysis of horizontal earth-air heat exchangers in a subtropical climate: An experimental study. Front. Built Environ. 8:981946. doi: 10.3389/fbuil.2022.981946.

[3] Sehli A, Hasni A, Tamali M. The potential of earth-air heat exchangers for low energy cooling of buildings in South Algeria. Energy Procedia. 2012;18:496–506.

[4] Mihalakakou G, Santamouris M, Asimakopoulos D. On the cooling potential of earth to air heat exchangers. Energy Convers Manag. 1994 May 1;35(5):395–402.

[5] Mihalakakou G, Lewis JO, Santamouris M. The influence of different ground covers on the heating potential of earth-to-air heat exchangers. Renew Energy. 1996 Jan 1;7(1):33–46.

[6] Ahmed SF, Amanullah MTO, Khan MMK, Rasul MG, Hassan NMS. Parametric study on thermal performance of horizontal earth pipe cooling system in summer. Energy Convers Manag. 2016 Apr 15;114:324–37.

[7] Rouag A, Benchabane A, Mehdid CE. Thermal design of Earth-to-Air Heat Exchanger. Part I a new transient semi-analytical model for determining soil temperature. J Clean Prod. 2018 May 1;182:538–44.

[8] Mehdid, C.E.; Benchabane, A.; Rouag, A.; Moummi, N.; Melhegueg, M.A.; Moummi, A.; Benabdi, M.L.; Brima, A. Thermal design of Earth-to-air heat exchanger. Part II a new transient semi-analytical model and experimental validation for estimating air temperature. *J. Clean. Prod.* 2018, *198*, 1536–1544..

[9] Krarti M, Kreider JF. Analytical model for heat transfer in an underground air tunnel. Energy Convers Manag. 1996 Oct 1;37(10):1561–74.

[10] De Paepe M, Janssens A. Thermo-hydraulic design of earth-air heat exchangers. Energy Build. 2003 May;35(4):389–97.

[11] Hollmuller P. Analytical characterisation of amplitude-dampening and phase-shifting in air/soil heat-exchangers. Int J Heat Mass Transf. 2003;46(22):4303–17.

[12] Badescu V. Simple and accurate model for the ground heat exchanger of a passive house. Renew Energy. 2007 Apr;32(5):845–55.

[13] Vaz J, Sattler MA, Dos Santos ED, Isoldi LA. Experimental and numerical analysis of an earth-air heat exchanger. Energy Build. 2011 Sep;43(9):2476–82.

[14] Aslam Bhutta MM, Hayat N, Bashir MH, Khan AR, Ahmad KN, Khan S. CFD applications in various heat exchangers design: A review. Appl Therm Eng. 2012;32(1):1–12.

[15] Wu H, Wang S, Zhu D. Modelling and evaluation of cooling capacity of earth–air–pipe systems. Energy Convers Manag. 2007 May 1;48(5):1462–71.

[16] Misra R, Bansal V, Agrawal G Das, Mathur J, Aseri TK. CFD analysis based parametric study of derating factor for Earth Air Tunnel Heat Exchanger. Appl Energy. 2013;103:266–77.

[17] Niu F, Yu Y, Yu D, Li H. Investigation on soil thermal saturation and recovery of an earth to air heat exchanger under different operation strategies. Appl Therm Eng. 2015;77:90–100.

[18] Laknizi A, Mahdaoui M, Anoune K, Bakhouya M, Abdellah A Ben, Oussous H. Parametric study and energy performance of an earth-air heat exchanger for a poultry house in Morocco. Vol. 8, International Journal of Renewable Energy Research. 2018. p. 2057–74.

[19] Kumar Verma M, Bansal V, Bihari Rana K. Development of Passive Energy Source As Earth Air Pipe Heat Exchangers (Eaphe) System -a Review. J Therm Eng. 2020 Oct 1;6(5):651–76.

[20] Ahmed ES, Hassan AS. The Impact of the Extreme Air Temperatures on the Characteristics of Iraq Weather *Iraqi Journal of Science, 2018, Vol. 59, No.2C, pp: 1139-1145 DOI:10.24996/ijs.2018.59.2C.19.*

[21] Mirianhosseinabadi S, Cho S, Kang EC, Lee EJ. Simulation modeling of Earth-To-Air Heat Exchanger (buried pipe) for the performance analysis of a School Building In Mid-Atlantic region. 2014 ASHRAE/IBPSA-USA Build Simul Conf. 2014;378–85.

[22] Holman, J.P. Heat Transfer. 10th Edition, McGraw-Hill, New York. (2009).

[23] Athieniti AK, Santamouris M. Thermal analysis and design of passive solar buildings. Therm Anal Des Passiv Sol Build. 2013;1–288.

[24] Singh SP. Optimization of earth-air tunnel system for space cooling. Energy Convers Manag. 1994 Aug 1;35(8):721–5.

[25] Lemmon EW, Jacobsen RT. Viscosity and thermal conductivity equations for nitrogen, oxygen, argon, and air. Int J Thermophys. 2004;25(1):21–69.

[26] Cengel, Y.A. and Cimbala, J.M. (2014) Fluid Mechanics. Fundamentals and Applications. 3rd Edition. McGraw-Hill, New York.